

# OPTIMIZATION OF MACHINING PERFORMANCE IN DRY END MILLING OF INCONEL 601

Vukelic, D.<sup>\*,#</sup>; Milosevic, A.<sup>\*</sup>; Kanovic, Z.<sup>\*</sup>; Sokac, M.<sup>\*</sup>; Santosi, Z.<sup>\*</sup> & Simunovic, G.<sup>\*\*</sup>

<sup>\*</sup> University of Novi Sad, Faculty of Technical Sciences, Trg Dositeja Obradovica 6, Novi Sad, Serbia

<sup>\*\*</sup> University of Slavonski Brod, Mechanical Engineering Faculty, Trg Ivane Brlic Mazuranic 2, Slavonski Brod, Croatia

E-Mail: vukelic@uns.ac.rs (<sup>#</sup> Corresponding author)

## Abstract

This study investigates the influence of helix angle, cutting speed, feed per tooth, radial depth of cut and axial depth of cut on surface roughness and material removal rate during dry end milling of Inconel 601. An I-optimal design of experiments was employed to develop a quadratic regression-based simulation model for surface roughness, while material removal rate was determined analytically. Multi-objective optimization was performed to maximize material removal rate while satisfying target surface roughness levels corresponding to previously defined machining quality grades. The results indicate that higher helix angles, moderate cutting speeds, lower feed per tooth and lower depths of cut lead to improved surface roughness. Conversely, a reduction in the stringency of surface roughness requirements enables a significant increase in productivity by permitting the use of more aggressive milling parameters, including higher cutting speeds, feed per tooth and depths of cut. Confirmation experiments demonstrated good agreement between predicted and measured surface roughness values, with low prediction errors, confirming high predictive accuracy and model stability.

(Received in April 2026, accepted in May 2026. This paper was with the authors 2 weeks for 2 revisions.)

**Key Words:** End Milling, Dry Conditions, Surface Roughness, Material Removal Rate

## 1. INTRODUCTION

Inconel alloys are widely recognized for their excellent high-temperature strength and corrosion resistance. However, these properties also make them difficult-to-cut due to low thermal conductivity, high hot hardness and strong chemical affinity with cutting tool materials, resulting in elevated cutting temperatures, accelerated tool wear and reduced productivity [1-3]. Consequently, Inconel alloys are commonly machined under wet conditions or using alternative cooling and lubrication strategies, such as cryogenic [4] and minimum quantity lubrication [5] techniques.

Milling is a widely used material removal process for producing surfaces with high dimensional accuracy and satisfactory surface quality. Dry milling of difficult-to-cut materials such as Inconel alloys remains particularly challenging. Nevertheless, dry machining offers important environmental, economic and operational advantages. Therefore, efficient dry machining requires careful selection of cutting tools and milling parameters, supported where appropriate by simulation, modelling and optimization approaches [6-8].

End milling is commonly applied for machining complex geometries such as slots, cavities and contoured surfaces. Several studies have investigated dry end milling of Inconel alloys from different perspectives. Wang et al. [9] identified optimal surface quality at high cutting speed and low feed per tooth and cutting depths. Motorcu et al. [10] showed that cutting speed strongly affects tool life, while coated tools significantly improve wear resistance. Sarkar et al. [11] identified depth of cut as the dominant factor affecting surface roughness. Grguraš et al. [12] demonstrated superior tool life of ceramic end mills under dry conditions. Kamdani et al. [13] reported increased flank wear with increasing cutting speed and radial depth of cut. Mohd Nor et al. [14] analysed the relationship between spindle speed, feed per tooth, cutting force and residual stress. Rajguru and Vasudevan [15] identified feed per tooth and radial depth of cut as

the most influential parameters affecting surface roughness. Finally, Rajguru and Vasudevan [16] reported that the minimum micro-hardness occurs at higher feed per tooth, lower cutting speed, greater depth of cut and a positive radial rake angle.

Effective end milling of Inconel alloys requires a systematic approach combining process modelling and optimization. Simulation and modelling techniques – such as finite element analysis [17], analytical [18] and empirical [19] modelling, and artificial neural networks [20] – predict key response variables like cutting forces, temperature, tool wear, surface roughness, etc. Optimization methods, including the Taguchi method [21], grey relational analysis [22], genetic algorithms [23] and particle swarm optimization [24], as well as other multi-objective optimization approaches applied in intelligent manufacturing systems [25], identify the best combination of input factors to maximize productivity, tool life, surface quality, etc. Integrating simulation-based modelling with optimization enables predictive, adaptive machining strategies, reducing trial-and-error and improving both economic and environmental efficiency [26].

Although extensive research has been conducted on the dry end milling of Inconel alloys, most existing studies primarily focus on the effects of milling parameters on responses. The influence of tool geometry parameters remains insufficiently explored in combination with milling conditions, especially when both surface quality and productivity are considered simultaneously. In addition, many reported optimization approaches rely on extremum-based solutions without explicitly considering the practical technological constraints associated with surface roughness classes, such as machining quality grades. As a result, the obtained optimal conditions often lack direct engineering interpretability and have limited applicability in process planning.

The aim of this study is to develop regression-based simulation models to describe the effects of helix angle, cutting speed, feed per tooth, radial depth of cut and axial depth of cut on surface roughness ( $Ra$ ). Furthermore, multi-objective optimization is applied to determine the optimal machining conditions that simultaneously enhance surface quality and productivity in dry end milling of Inconel alloys. Unlike the classical optimization problem, which seeks to minimize  $Ra$  while maximizing material removal rate ( $MRR$ ), this study formulates the optimization problem to maximize  $MRR$  and minimize the deviation from the target  $Ra$  value simultaneously. In other words, the problem reduces to determining the optimal input factors that maximize  $MRR$  while ensuring that  $Ra$  meets or falls below the required value, reflecting practical engineering considerations.

## **2. METHODOLOGY**

The research methodology employed in this study integrates experimental design, milling experiments, measurement and calculation, analysis, simulation modelling and optimization. The overall framework is presented in Fig. 1. The experimental investigation was performed on Inconel 601 workpieces (300×70×30 mm) using a vertical machining centre (Makino PS95). Solid end mills with five cutting edges and 20 mm diameter were used, coated with PVD TiAlN+TiSiN. Tool geometry included 5 flutes and 50 mm effective cutting length. The substrate was high-carbon steel. The radial and axial rake angles were both 5°. Five input factors were varied at three levels: helix angle ( $\lambda = 35, 40$  and  $45^\circ$ ), cutting speed ( $v_c = 20, 30$  and  $40$  m/min), feed per tooth ( $f_z = 0.03, 0.05$  and  $0.07$  mm/tooth), radial depth of cut ( $a_e = 0.5, 1$  and  $1.5$  mm) and axial depth of cut ( $a_p = 0.5, 1$  and  $1.5$  mm). The ranges of the input factor levels were determined based on published literature, preliminary experimental trials and cutting tool manufacturer recommendations. A relatively wider range of machining parameters was intentionally selected to enable a more detailed investigation of their effects on the response variables.

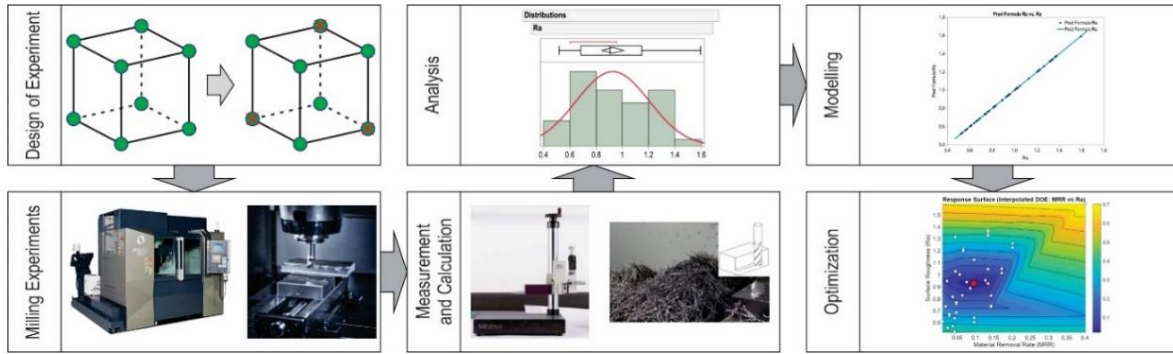


Figure 1: Research methodology.

In the study, two response variables were considered, the  $Ra$  parameter was measured, while the  $MRR$  was calculated.  $Ra$  was measured using the SurfTest SJ 410 device. The measurements were taken under the following parameters: probe tip radius of  $2 \mu\text{m}$ , measuring force of  $0.75 \text{ mN}$ , measuring speed of  $0.1 \text{ mm/s}$ , Gaussian filter, sampling length of  $0.8 \text{ mm}$ , evaluation length of  $4 \text{ mm}$  and stylus travel of  $4.8 \text{ mm}$ .  $MRR$  in end milling is defined as the volume of material removed per unit time and is defined as [27]:

$$MRR = a_e \cdot a_p \cdot v_f = a_e \cdot a_p \cdot f_z \cdot n \cdot z = a_e \cdot a_p \cdot f_z \cdot \frac{v_c}{\pi \cdot D_c} \cdot z \quad (1)$$

where:  $v_f$  is the table feed ( $\text{mm/min}$ ),  $n$  is the spindle speed ( $\text{rpm}$ ),  $z$  is the number of teeth and  $D_c$  is the cutting tool diameter ( $\text{mm}$ ).  $MRR$  was determined analytically and not modelled, as its functional dependence on the input factors is explicitly defined.

To investigate the influence of input factors, an experimental plan was defined using the design of experiments methodology. The experimental design enabled the evaluation of main effects, quadratic terms and interactions between input factors on  $Ra$ . An I-optimal experimental design was applied, as it is particularly suitable for predictive model development by minimising the average prediction variance within the observed experimental space. During the design development, several alternative experimental design configurations were analysed and a final set of 42 experimental runs was defined. This selection represents a compromise between the reliability of the predictive model and the efficiency, that is, the cost of conducting experiments.

Following the execution of the experimental plan, the collected data were subjected to analysis to quantify the relationships between input factors and the responses. The primary objective of this step was to identify significant factors and to capture the underlying process behaviour governing  $Ra$ . An empirical modelling approach based on multiple regression analysis was adopted. A quadratic response surface model was selected in order to account for nonlinear effects and potential interactions between input factors. The model enables prediction and optimization of  $Ra$  based on input parameters. Model parameters were estimated using the least squares method. The adequacy and statistical significance of the developed model were evaluated using analysis of variance (ANOVA), the coefficient of determination ( $R^2$ ), adjusted  $R^2$ , root mean square error ( $RMSE$ ) and residual diagnostics. Residual plots were used to verify model assumptions. The relative importance of model terms was assessed using the effect summary, while parameter influence was evaluated using scaled estimates. Model evaluation and validation were further performed by comparing predicted and experimental values. In addition, model robustness and parameter selection were investigated using K-fold cross-validation combined with adaptive Lasso regression, where the solution path was analysed to observe the effect of the penalization parameter on coefficient shrinkage and variable selection.

Based on the developed model, a multi-objective optimization problem was formulated to determine optimal dry end milling conditions. The objective is to maximize  $MRR$  while ensuring that  $Ra$  satisfies predefined quality requirements. A penalty-based formulation was

introduced to handle constraints related to allowable  $Ra$  levels. The resulting optimization problem is characterized by nonlinear relationships, conflicting objectives and a combination of continuous (cutting speed, feed per tooth, radial depth of cut and axial depth of cut) and categorical (helix angle) variables. Such a formulation enables systematic exploration of the trade-off between  $Ra$  and  $MRR$ , providing practical guidance for process parameter selection under different machining requirements.

### **3. EXPERIMENTAL RESULTS**

Table I presents the results of the experimental study.

Table I: Experimental results.

No.	$\lambda$ (°)	$v_c$ (m/min)	$f_z$ (mm/tooth)	$a_e$ (mm)	$a_p$ (mm)	$Ra$ ( $\mu\text{m}$ )	$MRR$ ( $\text{mm}^3/\text{s}$ )
1	45	40	0.05	1	1	0.955	2.654
2	40	30	0.05	1	1	0.641	1.990
3	45	40	0.07	1.5	0.5	1.341	2.787
4	40	40	0.07	1.5	0.5	1.370	2.787
5	40	30	0.05	1.5	1	0.743	2.986
6	45	30	0.07	1	1	0.928	2.787
7	35	40	0.03	1.5	0.5	0.989	1.194
8	35	20	0.05	1	1	0.842	1.327
9	35	40	0.07	1.5	1.5	1.595	8.360
10	45	40	0.03	0.5	0.5	0.752	0.398
11	45	40	0.07	0.5	1.5	1.338	2.787
12	35	30	0.05	1.5	1	0.812	2.986
13	45	30	0.03	1.5	0.5	0.530	0.896
14	35	40	0.07	0.5	0.5	1.298	0.929
15	40	20	0.07	0.5	1	1.039	0.929
16	35	30	0.03	0.5	1.5	0.628	0.896
17	45	20	0.07	1.5	1.5	1.227	4.180
18	40	30	0.05	1	1.5	0.718	2.986
19	40	20	0.07	1.5	1.5	1.263	4.180
20	45	30	0.05	1	1	0.589	1.990
21	35	30	0.07	1	1	1.067	2.787
22	40	40	0.07	0.5	1.5	1.342	2.787
23	45	20	0.05	0.5	1.5	0.772	0.995
24	45	20	0.07	0.5	0.5	0.931	0.464
25	35	20	0.03	1.5	1.5	0.904	1.791
26	35	20	0.07	1.5	0.5	1.197	1.393
27	35	20	0.03	0.5	0.5	0.629	0.199
28	40	40	0.03	0.5	1	0.798	0.796
29	45	30	0.03	0.5	1.5	0.537	0.896
30	40	40	0.03	1	0.5	0.829	0.796
31	40	20	0.07	1	0.5	1.014	0.929
32	35	40	0.05	0.5	1.5	1.143	1.990
33	40	20	0.03	0.5	1.5	0.641	0.597
34	35	40	0.03	1	1	0.958	1.592
35	40	40	0.03	1.5	1.5	1.031	3.583
36	35	30	0.05	1	0.5	0.703	0.995
37	40	20	0.03	1.5	0.5	0.659	0.597
38	40	30	0.05	0.5	0.5	0.576	0.498
39	45	20	0.05	1.5	0.5	0.758	0.995
40	45	40	0.03	1.5	1.5	1.032	3.583
41	35	20	0.07	0.5	1.5	1.186	1.393
42	45	20	0.03	1	1	0.588	0.796

Based on the obtained data, it can be concluded that the values of  $Ra$  and  $MRR$  vary depending on the combination of input factors.  $Ra$  ranged from  $0.530 \mu\text{m}$  to  $1.595 \mu\text{m}$ , while  $MRR$  varied from  $0.199 \text{ mm}^3/\text{s}$  to  $8.360 \text{ mm}^3/\text{s}$ , indicating substantial influence of input factors on process responses.

## 4. MODELLING RESULTS

### 4.1 Model development

Process modelling was performed using multiple regression analysis with parameters estimated by least squares. A quadratic response surface model was used to capture nonlinear effects:

$$Ra = \beta_0 + \sum \beta_i X_i + \sum \beta_{ii} X_i^2 + \sum \sum \beta_{ij} X_i X_j + \varepsilon \quad (2)$$

where  $X_i$  and  $X_j$  represent the input factors,  $\beta_0$  is the intercept term,  $\beta_i$ ,  $\beta_{ii}$  and  $\beta_{ij}$  are regression coefficients corresponding to the linear, quadratic and interaction effects, respectively, and  $\varepsilon$  is the random error term.

Preliminary screening indicated that interaction terms had  $p$ -values above the significance threshold and a negligible contribution to model fit; therefore, they were excluded from the final model. The regression coefficients were estimated based on experimental data, with a quadratic model fitted in order to minimize the mean squared error. In this way, the following regression equation was obtained, describing the dependence of  $Ra$  on the input factors:

$$Ra = 2.2822 - 0.0683 \cdot a_p - 0.1247 \cdot v_c - 11.8629 \cdot f - 0.0495 \cdot a_e + 0.1013 \cdot a_p^2 + 0.0023 \cdot v_c^2 + 231.5149 \cdot f^2 + 0.0950 \cdot a_e^2 + \begin{cases} 0.0704, & \lambda = 35^\circ \\ -0.0213, & \lambda = 40^\circ \\ -0.0491, & \lambda = 45^\circ \end{cases} \quad (3)$$

The model quantifies linear and nonlinear effects of input parameters on  $Ra$ . Linear effects in the model represent the dominant trends in input factor influence, while quadratic effects indicate deviations from linear behaviour within the analysed range.

### 4.2 Model analysis

The statistical significance and reliability of the developed regression model were evaluated using ANOVA (Table II). The ANOVA results show that the regression model is statistically significant, with a high  $F$ -ratio (1401.329) and a corresponding  $p$ -value below the significance threshold ( $p < 0.05$ ). The low mean square error (0.0002) further supports the model's accuracy.

Table II: Analysis of variance.

Source	DF	Sum of squares	Mean square	F-ratio	p-value
Model	10	3.0752	0.3075	1401.329	<0.0001
Error	31	0.0068	0.0002	–	–
C. Total	41	3.0820	–	–	–

The obtained values ( $R^2 = 0.9977$ , adjusted  $R^2 = 0.9971$ ) indicate that the model explains more than 99.7% of the variability in  $Ra$ . The low root mean squared error ( $RMSE = 0.0148 \mu\text{m}$ ) further confirms the high prediction accuracy relative to the mean experimental  $Ra$  value of  $0.926 \mu\text{m}$ .

The relative importance of individual model terms was assessed using effect summary (sorted by  $\text{LogWorth} = -\log_{10}(p\text{-value})$ ). The  $\text{LogWorth}$  values and corresponding  $p$ -values show that all linear and quadratic effects are statistically significant at the  $p < 0.05$  level (Table III). Feed per tooth was identified as the most influential factor, followed by cutting speed and its quadratic term. Other significant factors included radial and axial depth of cut, helix angle,

and the quadratic terms of feed per tooth, axial depth of cut and radial depth of cut, confirming that both linear and nonlinear effects significantly influence  $Ra$  variation.

Table III: Effect summary.

Source	LogWorth	$p$ -value
$f_z$	37.229	0.0000
$v_c$	29.175	0.0000
$v_c \times v_c$	27.445	0.0000
$a_e$	21.757	0.0000
$a_p$	21.029	0.0000
$\lambda$	19.112	0.0000
$f_z \times f_z$	15.903	0.0000
$a_p \times a_p$	3.593	0.0003
$a_e \times a_e$	3.241	0.0006

Table IV: Scaled estimates.

Term	Estimate	Std. error	$t$ -ratio	$p$ -value
$f_z$	11.2885	0.1362	82.86	<0.0001
$v_c$	0.0123	0.0003	45.32	<0.0001
$v_c \times v_c$	0.0023	$5.741 \cdot 10^{-5}$	39.77	<0.0001
$a_e$	0.1405	0.0055	25.74	<0.0001
$a_p$	0.1343	0.0055	24.32	<0.0001
$\lambda$ (35°)	0.0704	0.0032	21.79	<0.0001
$f_z \times f_z$	231.5149	14.3530	16.13	<0.0001
$\lambda$ (40°)	-0.0213	0.0032	-6.61	<0.0001
$a_p \times a_p$	0.1013	0.0245	4.13	0.0003
$a_e \times a_e$	0.0950	0.0248	3.84	0.0006

Scaled estimates (Table IV) were used to compare the relative influence of input factors independently of their units and variation ranges. The results show that feed per tooth has the greatest effect on  $Ra$ , followed by cutting speed, radial depth of cut, axial depth of cut and helix angle. The scaled quadratic terms additionally confirm nonlinear process behaviour.

### 4.3 Model validation

The developed regression-based simulation model was validated to assess its predictive accuracy and generalisation capability within the defined experimental space.

Validation was conducted by comparing experimentally obtained values with model-predicted values (Fig. 2). The points are distributed close to the line of equality, indicating good agreement between the model and the experimental results.

Further model validation was conducted through residual analysis. Fig. 3 shows the relationship between residuals and predicted values, where a random scatter without any systematic pattern is observed, indicating the adequacy of the selected model and homoscedasticity of variance.

Studentized residuals (Fig. 4) do not display extreme deviations or pronounced outliers, confirming model stability and the absence of highly influential observations that could distort the regression coefficients.

The normal quantile plot of residuals (Fig. 5) shows an approximately linear distribution of points, indicating that the residuals follow a normal distribution. These diagnostic results confirm the adequacy of the regression model.

To assess the reliability of the developed model, validation was conducted using K-fold cross-validation, in which the dataset was divided into 10 subsets and the model was iteratively trained and tested on different data segments. During validation, an adaptive Lasso regression approach was applied, allowing simultaneous parameter estimation and selection of significant factors. Fig. 6 presents the solution path diagram, which shows the variation of model coefficients as a function of the penalisation parameter. As penalisation increases, the number of active parameters gradually decreases, leaving only the most influential factors in the model. The validation results show that the model maintains high values of the coefficient of determination ( $R^2 = 0.998$  and adjusted  $R^2 = 0.998$ ), along with a low root mean squared error ( $RMSE = 0.0022$ ), confirming high predictive accuracy on the validation datasets. Comparison between training and validation results does not show significant deviations, indicating stable generalisation performance and the absence of overfitting.

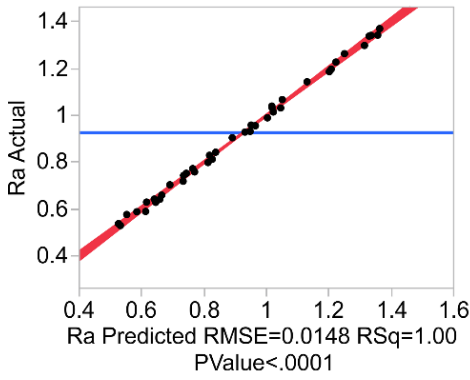


Figure 2: Actual by predicted plot.

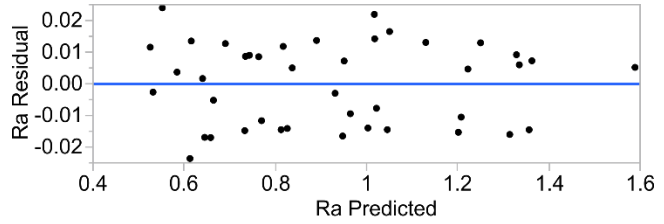


Figure 3: Residual by predicted plot.

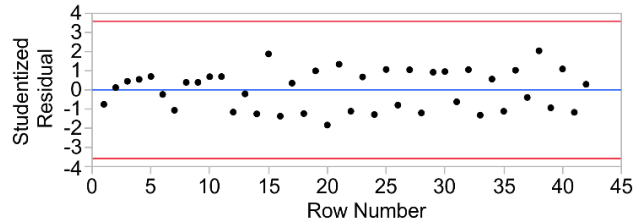


Figure 4: Studentized residuals.

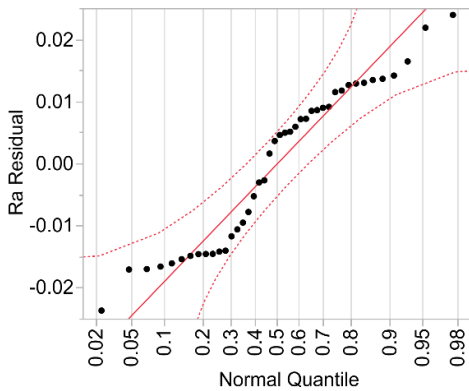


Figure 5: Residual normal quantile plot.

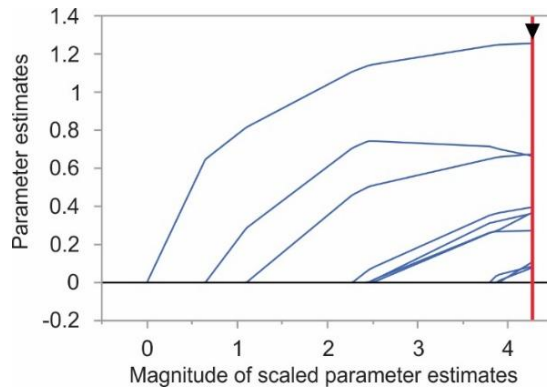


Figure 6: Solution path.

Fig. 7 presents the prediction profiler illustrating the influence of input factors on  $Ra$ . This figure highlights the relative influence of helix angle, cutting speed, feed per tooth and depths of cut on  $Ra$ , providing an intuitive complement to the statistical analyses presented above. The profiler confirms the trends observed in the ANOVA and residual analyses, showing that feed per tooth has the strongest impact, followed by cutting speed and its quadratic effect, consistent with the reported significance levels. By integrating both statistical validation and visual interpretation, the model demonstrates robustness, predictive reliability and clear representation of process behaviour across the investigated domain.

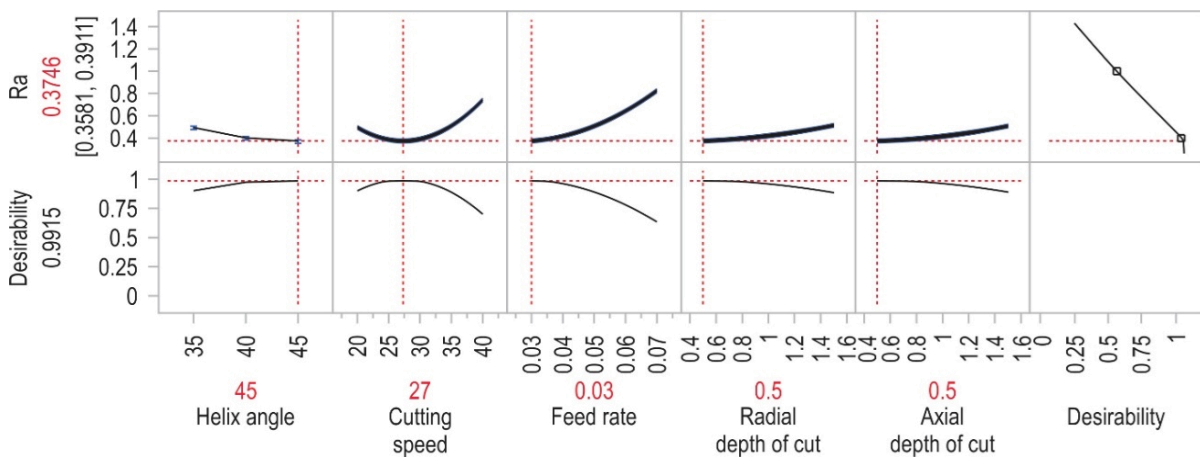


Figure 7: Prediction profiler.

At the minimum predicted  $Ra$  condition, the model predicts a  $Ra$  value of  $0.3746 \mu\text{m}$  (95 % confidence interval:  $0.3581\text{--}0.3911 \mu\text{m}$ ). The corresponding desirability value reaches 0.9915, indicating near-ideal minimization of  $Ra$  within the investigated experimental region. The helix angle shows that  $Ra$  decreases with increasing helix angle and the lowest  $Ra$  is achieved at the upper limit of the range ( $\lambda=45^\circ$ ). Cutting speed exhibits a mild quadratic (U-shaped) relationship, with the minimum  $Ra$  located at  $v_c=27 \text{ m/min}$ . Feed per tooth was identified as the most influential factor, since  $Ra$  increases sharply with higher feed per tooth, making the optimum at the lowest investigated value ( $f_z=0.03 \text{ mm/tooth}$ ). Both the radial depth of cut and the axial depth of cut exhibit a mild linear effect, with the lowest  $Ra$  values obtained at the minimum depths of cut ( $a_e = a_p = 0.5 \text{ mm}$ ).

## 5. OPTIMIZATION RESULTS

The optimization problem was formulated to simultaneously achieve a target  $Ra$  and maximize the  $MRR$ , thereby ensuring an appropriate trade-off between surface quality and process productivity. The optimization problem is defined as minimisation of the following objective function:

$$F = w_{Ra} \cdot f_{Ra} + w_{MRR} \cdot (1 - MRR_n) \quad (4)$$

where  $w_{Ra}$  and  $w_{MRR}$  are weighting coefficients that define the relative importance of  $Ra$  and  $MRR$ , respectively,  $f_{Ra}$  denotes the penalty-based term associated with  $Ra$ , while  $MRR_n$  denotes the normalized  $MRR$ . Because the response variables have different physical units and variation ranges, min-max normalization was applied. The normalized values of  $Ra$  and  $MRR$  were defined within the interval  $[0, 1]$  using the following expressions:

$$Ra_n = (Ra - Ra_{min}) / (Ra_{max} - Ra_{min}) \quad (5)$$

$$MRR_n = (MRR - MRR_{min}) / (MRR_{max} - MRR_{min}) \quad (6)$$

This procedure ensures that both criteria contribute equally to the objective function, preventing dominance due to differing numerical scales. To incorporate the target  $Ra$  requirement, a penalty-based formulation was defined for the  $Ra$  term as:

$$f_{Ra} = Ra_{ref} - Ra_{act}, Ra_{act} \leq Ra_{ref} \quad (7)$$

$$f_{Ra} = c \cdot Ra_{act}, Ra_{act} > Ra_{ref} \quad (8)$$

where  $Ra_{act}$  is the actual predicted  $Ra$ ,  $Ra_{ref}$  represents the target value of  $Ra$ , and  $c$  is a penalty coefficient that increases the cost of solutions violating the specified  $Ra$  requirement. This formulation ensures smooth penalization of deviations from the target value while strongly discouraging solutions that exceed the allowable roughness limit.

To analyse the influence of required  $Ra$  on optimal solutions in greater detail, optimization was conducted for three  $Ra$  levels corresponding to machining quality grades N5, N6 and N7. For each scenario, a target value of  $Ra$  value was defined, while  $MRR$  was treated as a maximization criterion. The considered scenarios are:

- N5 – the most stringent  $Ra$  requirement ( $Ra \leq 0.4 \mu\text{m}$ ), corresponding to fine finishing operations where minimal  $Ra$  is emphasised;
- N6 – a moderate  $Ra$  level ( $Ra \leq 0.8 \mu\text{m}$ ), balancing  $Ra$  and  $MRR$ ;
- N7 – the least strict requirement ( $Ra \leq 1.6 \mu\text{m}$ ), prioritising higher  $MRR$  with an acceptable increase in  $Ra$ .

The multi-objective optimization of the dry end milling process was carried out using a genetic algorithm. The algorithm was executed with a population size of 100, a crossover fraction of 0.8 and a mutation rate of 0.02 for 400 generations. The parameter values were selected through a trial-and-error procedure to achieve satisfactory convergence and solution stability. The resulting optimal input factors and response variables are presented in Table V.

Table V: Optimization results.

Scenario	Condition	$\lambda$ (°)	$v_c$ (m/min)	$f_z$ (mm/tooth)	$a_e$ (mm)	$a_p$ (mm)	$Ra$ ( $\mu\text{m}$ )	$MRR$ ( $\text{mm}^3/\text{s}$ )
Scenario 1	$Ra \leq 0.4 \mu\text{m}$ $MRR = MRR_{max}$	45	28	0.03	0.6	0.7	0.392	0.468
Scenario 2	$Ra \leq 0.8 \mu\text{m}$ $MRR = MRR_{max}$	45	30	0.05	1.4	1.5	0.777	4.180
Scenario 3	$Ra \leq 1.6 \mu\text{m}$ $MRR = MRR_{max}$	35	40	0.07	1.5	1.5	1.587	8.360

## 6. CONFIRMATION RESULTS

Three additional confirmation experiments were conducted using the optimal input parameters obtained from the optimization procedure (Table V). Model performance was evaluated by comparing predicted and measured  $Ra$  values (Table VI). The absolute error ( $AE$ ) ranges from 0.005 to 0.017  $\mu\text{m}$ , while the percentage error ( $PE$ ) varies between 0.626 % and 2.141 %. The mean  $AE$  and  $PE$  errors are 0.011  $\mu\text{m}$  and 1.342 %, respectively. The low and consistent error values indicate good predictive accuracy and stable model behaviour without significant outliers.

Table VI: Confirmation results.

Scenario	$Ra$ predicted ( $\mu\text{m}$ )	$Ra$ measured ( $\mu\text{m}$ )	$AE$ ( $\mu\text{m}$ )	$PE$ (%)
Scenario 1	0.392	0.397	0.005	1.259
Scenario 2	0.777	0.794	0.017	2.141
Scenario 3	1.587	1.597	0.010	0.626

## 7. DISCUSSION

The developed regression-based simulation model, supported by analysis and validation results, provides a basis for interpreting the influence of tool geometry and milling parameters on  $Ra$  and  $MRR$ . The observed trends are consistent with the statistical significance ranking obtained from the regression model.

$Ra$  improves with increasing helix angle, although this parameter exhibits a relatively lower influence compared to the dominant machining parameters identified in the ANOVA results. This improvement can be attributed to increased sharpness and more favourable cutting edge engagement, which reduce cutting resistance and promote smoother chip formation. In addition, a higher helix angle facilitates gradual tool entry and improves chip evacuation by directing chips more efficiently along the flute. These effects contribute to reduced vibration and more stable cutting conditions, ultimately leading to improved  $Ra$ . According to the regression and ANOVA results, feed per tooth is the most influential parameter on  $Ra$ . Increasing feed per tooth deteriorates  $Ra$  due to the formation of higher peaks and deeper valleys on the machined surface. This is accompanied by an increase in chip thickness, which results in higher cutting forces and elevated cutting temperatures. In dry end milling of Inconel alloys, these effects are further intensified due to poor heat dissipation and the material's tendency to work harden, leading to accelerated tool wear and further surface degradation. As cutting speed increases,  $Ra$  initially improves due to reduced friction, reduced built-up edge formation, and more stable cutting conditions. However, at higher cutting speeds, an increase in  $Ra$  is observed, indicating a nonlinear (quadratic) effect of cutting speed on  $Ra$ . This behaviour is associated with the transition from friction-dominated to thermally-dominated cutting conditions, where increased cutting temperatures accelerate tool wear. In dry end milling of Inconel alloys, this effect is

further intensified due to limited heat dissipation, resulting in rapid thermal loading in the cutting zone and degradation of  $Ra$ . Increasing radial and axial depths of cut leads to an increase in  $Ra$ . This is primarily due to an increase in the uncut chip cross-sectional area, which results in higher cutting forces and greater heat generation. In dry end milling conditions, limited heat dissipation intensifies thermal loading in the cutting zone, while the work-hardening behaviour of Inconel alloys further increases cutting resistance. These combined effects accelerate tool wear and promote vibration during machining, ultimately contributing to poorer  $Ra$ .

The optimization results reveal a clear trade-off between  $Ra$  and  $MRR$  in dry end milling of Inconel 601. As the  $Ra$  constraint is progressively increased from N5 to N7, the feasible region for  $MRR$  maximization expands. For N5 ( $Ra \leq 0.4 \mu\text{m}$ ),  $MRR$  is  $0.468 \text{ mm}^3/\text{s}$  and the solution favours conservative parameters with low feed per tooth and lower depths of cut, prioritizing surface quality over productivity. For N6 ( $Ra \leq 0.8 \mu\text{m}$ ),  $MRR$  increases to  $4.180 \text{ mm}^3/\text{s}$ , reflecting a balanced compromise achieved through moderate increases in feed per tooth, cutting speed, and depths of cut. This improvement is associated with the lower sensitivity of  $Ra$  to depth of cut compared to feed per tooth and cutting speed. For N7 ( $Ra \leq 1.6 \mu\text{m}$ ),  $MRR$  reaches  $8.360 \text{ mm}^3/\text{s}$ , where higher levels of all machining parameters shift the process towards productivity-driven conditions. These results indicate that the proposed optimization framework does not yield a single optimum, but a set of solutions depending on  $Ra$  requirements. This provides flexibility for selecting machining conditions based on production requirements.

The obtained confirmation results indicate good agreement between predicted and measured  $Ra$  values across all experiments. No increasing error trend is observed, indicating stable model performance across the investigated range. This confirms good generalization capability of the model. From an engineering perspective, the observed error levels are sufficiently low for practical application.

## **8. CONCLUSIONS**

This study investigated the influence of tool geometry and milling parameters on  $Ra$  and  $MRR$  in dry end milling of Inconel 601 using regression modelling and multi-objective optimization. A quadratic regression model was developed and validated with high predictive accuracy within the experimental domain.

Feed per tooth was identified as the most influential factor on  $Ra$ , followed by cutting speed, radial depth of cut, axial depth of cut and helix angle. Improved  $Ra$  was achieved at higher helix angles, moderate cutting speeds and lower feed per tooth and depths of cut.

The proposed optimization framework enabled determination of machining conditions that maximize  $MRR$  while satisfying predefined  $Ra$  quality levels (N5–N7). Results confirmed a clear trade-off between productivity and surface quality, where relaxed  $Ra$  constraints led to significantly higher  $MRR$  and more aggressive milling conditions.

Validation experiments showed good agreement between predicted and measured  $Ra$  values, confirming model reliability and applicability. Overall, the results demonstrate that combined consideration of tool geometry and milling parameters can effectively support productivity- and quality-oriented dry machining of Inconel alloys.

Future research should extend the investigated milling parameters and tool geometry features to improve model generality. Additional responses such as cutting forces, temperature, and tool wear should be incorporated to better capture machining mechanisms. Comparative analysis of dry machining and various cooling/lubrication strategies is required to quantify their effect on the trade-off between surface quality and productivity. Finally, application of the proposed methodology to other difficult-to-cut alloys would strengthen its industrial applicability.

## **ACKNOWLEDGEMENT**

This research has been supported by the Ministry of Science, Technological Development and Innovation (Contract No. 451-03-34/2026-03/200156) and the Faculty of Technical Sciences, University of Novi Sad through project “Scientific and Artistic Research Work of Researchers in Teaching and Associate Positions at the Faculty of Technical Sciences, University of Novi Sad 2026” (No. 01-3609/1).

## **REFERENCES**

- [1] Wang, B.; Wang, Z.; Yin, Z.; Yuan, J. (2024). Wear behavior of ultrafine WC-Co cemented carbide end mills during milling of Inconel 718, *Wear*, Vols. 546-547, Paper 205359, 14 pages, doi:[10.1016/j.wear.2024.205359](https://doi.org/10.1016/j.wear.2024.205359)
- [2] Petru, J.; Zlamal, T.; Čep, R.; Sadilek, M.; Stančekova, D. (2017). The effect of feed rate on durability and wear of exchangeable cutting inserts during cutting Ni-625, *Technical Gazette*, Vol. 24, Suppl. 1, 1-6, doi:[10.17559/TV-20131221170237](https://doi.org/10.17559/TV-20131221170237)
- [3] Milosevic, A.; Simunovic, G.; Kanovic, Z.; Simunovic, K.; Kocovic, V.; Vukelic, D. (2025). Modelling and optimization of surface quality and productivity in turning Inconel 825 alloy, *International Journal of Simulation Modelling*, Vol. 24, No. 4, 565-576, doi:[10.2507/IJSIMM24-4-725](https://doi.org/10.2507/IJSIMM24-4-725)
- [4] Anburaj, R.; Pradeep Kumar, M.; Navin Kumar, B.; Ross, N. S. (2025). Enhancing machining performance of Inconel 625 through cryogenic cooling in face milling-EDAS optimization and AI prediction, *Materials and Manufacturing Processes*, Vol. 40, No. 10, 1365-1377, doi:[10.1080/10426914.2025.2507078](https://doi.org/10.1080/10426914.2025.2507078)
- [5] Kasim, M. S.; Hafiz, M. S. A.; Ghani, J. A.; Haron, C. H. C.; Izamshah, R.; Aziz, M. S. A.; Mohamad, W. N. F.; Wong, P. K.; Saedon, J. (2019). Chip morphology in ball nose end milling process of nickel-based alloy material under MQL condition, *The International Journal of Advanced Manufacturing Technology*, Vol. 103, Nos. 9-12, 4621-4625, doi:[10.1007/s00170-019-03948-z](https://doi.org/10.1007/s00170-019-03948-z)
- [6] Gao, H.; Shen, H.; Yue, C.; Li, R.; Liang, S. Y.; Wang, Y.; Liu, W.; Yang, Y. (2025). A monitoring method of milling chatter based on optimized hybrid neural network with attention mechanism, *Facta Universitatis, Series: Mechanical Engineering*, Vol. 23, No. 2, 227-250, doi:[10.22190/FUME240804047G](https://doi.org/10.22190/FUME240804047G)
- [7] Mao, J.; Tsuchiya, K.; Morigo, C.; Yukinari, S.; Tahara, H.; Kurashiki, Y. (2026). Reducing tool wear in high-speed milling of Inconel 718 by optimizing flank-face coolant direction: a CFD-supported approach toward sustainable machining, *Journal of Manufacturing Processes*, Vol. 160, 111-133, doi:[10.1016/j.jmapro.2026.01.065](https://doi.org/10.1016/j.jmapro.2026.01.065)
- [8] Feng, Y. T.; Shi, Z. R.; Yang, X.; Huang, W.; Luo, X.; Li, Y. H.; Yu, L. (2025). Optimizing abrasive water jet milling of alumina ceramics with RBF neural networks, *Advances in Production Engineering & Management*, Vol. 20, No. 3, 325-339, doi:[10.14743/APEM2025.3.543](https://doi.org/10.14743/APEM2025.3.543)
- [9] Wang, Y. W.; Zhang, S.; Li, J. F.; Ding, T. C. (2010). Optimal cutting parameters for desired surface roughness in end milling Inconel 718, *Advanced Materials Research*, Vols. 126-128, 911-916, doi:[10.4028/www.scientific.net/amr.126-128.911](https://doi.org/10.4028/www.scientific.net/amr.126-128.911)
- [10] Motorcu, A. R.; Kuş, A.; Arslan, R.; Tekin, Y.; Ezentas, R. (2013). Evaluation of tool life - tool wear in milling of Inconel 718 superalloy and the investigation of effects of cutting parameters on surface roughness with Taguchi method, *Technical Gazette*, Vol. 20, No. 5, 765-774
- [11] Sarkar, B.; Reddy, M. M.; Debnath, S. (2017). Effect of machining parameters on surface finish of Inconel 718 in end milling, *MATEC Web of Conferences*, Vol. 95, Paper 02009, 6 pages, doi:[10.1051/mateconf/20179502009](https://doi.org/10.1051/mateconf/20179502009)
- [12] Grguraš, D.; Kern, M.; Pušavec, F. (2018). Suitability of the full body ceramic end milling tools for high speed machining of nickel based alloy Inconel 718, *Procedia CIRP*, Vol. 77, 630-633, doi:[10.1016/j.procir.2018.08.190](https://doi.org/10.1016/j.procir.2018.08.190)
- [13] Kamdani, K.; Hasan, S.; Ashaary, A.F.I.A.; Lajis, M. A.; Rahim, E. A. (2019). Study on tool wear and wear mechanisms of end milling nickel-based alloy, *Jurnal Tribologi*, Vol. 21, 82-92

- [14] Mohd Nor, N. A.; Baharudin, B. T. H. T.; Leman, Z.; Mohd Ariffin, M. K. A. (2022). Correlation between cutting force and residual stress in dry end-milling of Inconel HX, *International Journal of Integrated Engineering*, Vol. 14, No. 6, 47-54, doi:[10.30880/ijie.2022.14.06.005](https://doi.org/10.30880/ijie.2022.14.06.005)
- [15] Rajguru, R.; Vasudevan, H. (2022). Investigating the effect of cutting conditions and tool geometry on surface roughness in dry end milling of Inconel 625 using TiAlSiN ultra hard coated solid carbide tool, *Advances in Materials and Processing Technologies*, Vol. 8, Suppl. 1, 128-137, doi:[10.1080/2374068x.2020.1855964](https://doi.org/10.1080/2374068x.2020.1855964)
- [16] Rajguru, R.; Vasudevan, H. (2023). Impact of process parameters on machining-induced micro-hardness in dry end milling of Inconel 625 using coated tool, *Proceedings of the International Conference on Intelligent Manufacturing and Automation*, 511-518, doi:[10.1007/978-981-19-7971-2\\_49](https://doi.org/10.1007/978-981-19-7971-2_49)
- [17] Soo, S. L.; Dewes, R. C.; Aspinwall, D. K. (2010). 3D FE modelling of high-speed ball nose end milling, *The International Journal of Advanced Manufacturing Technology*, Vol. 50, Nos. 9-12, 871-882, doi:[10.1007/s00170-010-2581-y](https://doi.org/10.1007/s00170-010-2581-y)
- [18] Moufki, A.; Le Coz, G.; Dudzinski, D. (2017). End-milling of Inconel 718 superalloy – an analytical modelling, *Procedia CIRP*, Vol. 58, 358-363, doi:[10.1016/j.procir.2017.03.330](https://doi.org/10.1016/j.procir.2017.03.330)
- [19] Kumar, S.; Chandna, P.; Bhushan, G. (2021). Empirical modelling for workpiece temperature during end milling of Inconel 625 using a Green's function approach based on Dirac delta function, *Journal of Thermal Engineering*, Vol. 7, Suppl. 14, 1990-2000, doi:[10.18186/thermal.1051292](https://doi.org/10.18186/thermal.1051292)
- [20] Felusiak-Czyryca, A.; Twardowski, P. (2025). Prediction of tool wear based cutting forces during end milling of Inconel 718 using artificial neural networks, *Advances in Science and Technology Research Journal*, Vol. 19, No. 7, 394-405, doi:[10.12913/22998624/204203](https://doi.org/10.12913/22998624/204203)
- [21] Sathish, T.; Arul, K.; Subbiah, R.; Ravichandran, M.; Mohanavel, V. (2021). Optimization on end milling operating parameters for super alloy of Inconel 617 by Taguchi's L27 orthogonal array, *Journal of Physics: Conference Series*, Paper 012013, 13 pages, doi:[10.1088/1742-6596/2027/1/012013](https://doi.org/10.1088/1742-6596/2027/1/012013)
- [22] Sanghvi, N.; Vora, D.; Patel, J.; Malik, A. (2021). Optimization of end milling of Inconel 825 with coated tool: a mathematical comparison between GRA, TOPSIS and Fuzzy Logic methods, *Materials Today: Proceedings*, Vol. 38, Part 5, 2301-2309, doi:[10.1016/j.matpr.2020.06.413](https://doi.org/10.1016/j.matpr.2020.06.413)
- [23] Gaike, V.; Sahu, J.; Pawade, R. (2018). Optimization of cutting parameters for cutting force minimization in helical ball end milling of Inconel 718 by using genetic algorithm, *Procedia CIRP*, Vol. 77, 477-480, doi:[10.1016/j.procir.2018.08.261](https://doi.org/10.1016/j.procir.2018.08.261)
- [24] Zhou, J.; Ren, J.; Yao, C. (2017). Multi-objective optimization of multi-axis ball-end milling Inconel 718 via grey relational analysis coupled with RBF neural network and PSO algorithm, *Measurement*, Vol. 102, 271-285, doi:[10.1016/j.measurement.2017.01.057](https://doi.org/10.1016/j.measurement.2017.01.057)
- [25] Mou, J. B. (2024). Multi-objective optimization for resource allocation in intelligent manufacturing, *International Journal of Simulation Modelling*, Vol. 23, No. 2, 359-370, doi:[10.2507/IJSIMM23-2-CO9](https://doi.org/10.2507/IJSIMM23-2-CO9)
- [26] Rajguru, R.; Vasudevan, H. (2026). Investigation of surface roughness parameters under dry end milling of Inconel 625 with coated tool, *Proceedings of the Modeling and Simulation in Manufacturing (AIMTDR-2023)*, 55-64, doi:[10.1007/978-981-95-2535-5\\_5](https://doi.org/10.1007/978-981-95-2535-5_5)
- [27] Huda, Z. (2020). *Machining Processes and Machines: Fundamentals, Analysis, and Calculations*, 1<sup>st</sup> edition, CRC Press, Boca Raton, doi:[10.1201/9781003081203](https://doi.org/10.1201/9781003081203)